

MUON COOLING IN THE RFOFO RING*

R.C. Fernow, J.S. Berg, J.C. Gallardo, R.B. Palmer, BNL, Upton, NY 11973, USA

Dated: April 29, 2003

Abstract

Practical muon cooling rings could lead to better performance or lower cost designs of neutrino factories or muon colliders. The performance of the ring described here compares favorably with the linear cooling channel used in the second U.S. Neutrino Factory Study[1]. The 6D phase space density of an idealized ring is increased by a factor of 238, compared with the linear channel's factor of only 15. The simulations make use of fully realistic magnetic fields, and include absorber and rf cavity windows, and empty lattice cells for injection/extraction.

INTRODUCTION

In the present U.S. Neutrino Factory design [2] the muon beam 6D phase space density must be reduced in order to be able to accelerate it and inject into the storage ring pointing to a long distance neutrino detector. Ionization cooling is currently the only feasible option for cooling the beam within the muon lifetime ($\tau_0 = 2.19 \mu\text{s}$). If muons alternately pass through a material absorber, and are then reaccelerated, and if there is sufficient focusing at the absorber, then the muon's transverse phase space is reduced, *i.e.* the muons are cooled in the transverse dimension. A consequence of the transverse cooling is an increase of the longitudinal phase space caused by energy straggling in the material. The consequent momentum spread can be reduced if dispersion is introduced and a wedge absorber placed such that high momentum particles pass through more material than low momentum particles. However, in this process the beam width is increased. The process is thus primarily an exchange of emittance between the longitudinal and transverse dimensions, but when combined with transverse cooling in the material, all three dimensions can be cooled.

Recently there has been considerable progress in the design of cooling rings for neutrino factories and muon colliders[3]. The ring described here is based on an earlier design that used a simplified model of the magnetic field[4]. The ring consists of twelve 2.75 m long cells, each of which provide transverse cooling and emittance exchange. The focusing comes from a so-called RFOFO lattice of alternating direction solenoids, giving large angular and momentum acceptances. The axial magnetic field changes direction in the center of the cell. Ionization cooling is provided in 6D by sending the muon beam through wedge-shaped absorbers containing liquid H_2 . The energy

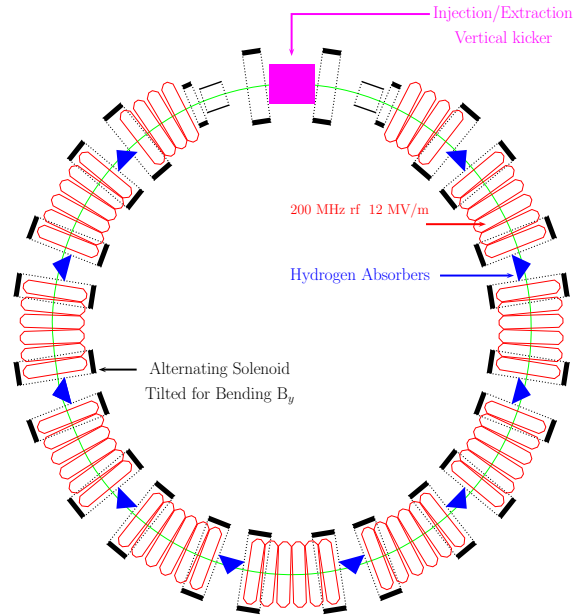


Figure 1: Layout of the RFOFO cooling ring.

lost in the absorbers is replaced using 201.25 MHz rf cavities in each lattice cell.

Figure 1 shows the layout of the cooling ring drawn to scale. The RFOFO lattice was chosen because, apart from questions of injection/extraction, all cells are strictly identical, and the presence of an integer betatron resonance within the momentum acceptance is eliminated. The ring design parameters are given in Tb. 1.

Table 1: RFOFO Basic Ring Parameters

Circumference (m)	33
Cells	12
Max B_z (T)	2.77
Coil Tilts (deg.)	3.0
Ave Momentum (MeV/c)	220
Min Trans. Beta (cm)	38
Max. Dispersion (cm)	8
Momentum Compaction	0.0037
Wedge Absorber Material	H_2
Wedge Thickness on axis (cm)	25.4
Wedge Angle ($^\circ$)	90
Wedge Vertex position (cm)	12.7
Wedge Azimuthal angle ($^\circ$)	230
Frequency (MHz)	201.25
Gradient (MV/m)	12
Phase ($^\circ$) from 0-crossing	25

* MUC-NOTE-COOL-THEORY-273

Figure 2 shows a detailed view of three cells of the lattice, in plan (a) and side (b) views. The solenoids are not

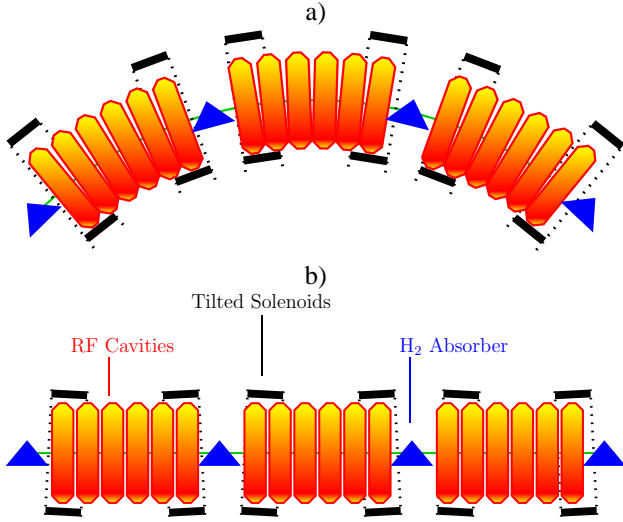


Figure 2: Three cells of the RFOFO lattice; a) plan view; b) side view. Notice that the coils have been displaced radially by 10 cm.

evenly spaced; those on either side of the absorbers are closer in order to increase the focusing at the absorber. The longitudinal field on-axis has an approximately sinusoidal dependence on position, as shown in Fig. 3. The beam axis is displaced laterally with respect to the coil centers (as shown in Fig. 2a) to minimize horizontal fields that cause vertical beam deviations.

Figure 4a) shows the beta function along a cell; the minimum value at the center of the absorber and at the central momentum is about 38 cm. Figure 4b) plots the beta function as a function of the muon beam momentum showing that the lattice transmits particles in the momentum band 160 - 260 MeV/c.

The bending field for the ring, and the required dispersion, are provided by alternately tilting the solenoids by 3.0° (as shown in Fig. 2b).

It is found that the acceptance is reduced as the bending field is increased. We thus use a wedge with maximum possible angle (giving zero thickness on one side), and the lowest bending field consistent with adequate emittance exchange. The dispersion at the absorber is approximately 8 cm in a direction 26° from the y axis. The dispersion at the center of the rf cavity region has the opposite sign, and is mostly in the y direction (see Fig. 5).

The rf cavities have a frequency of 201.25 MHz and an accelerating gradient of 12 MV/m.

MODELING THE RING

The RFOFO ring was modeled using the ICOOL code[5]. The magnetic field from the tipped solenoids was calculated in an independent code that found the resul-

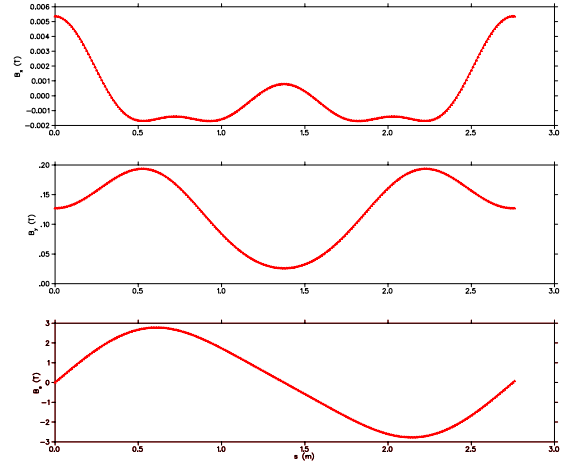
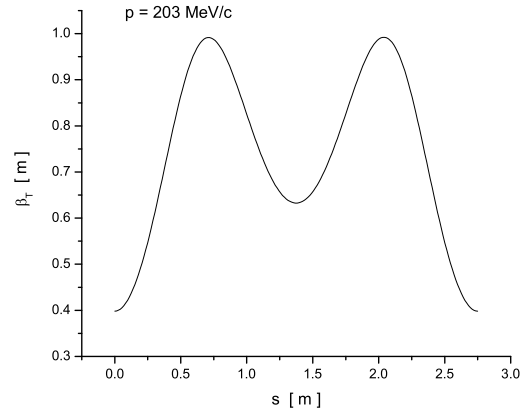
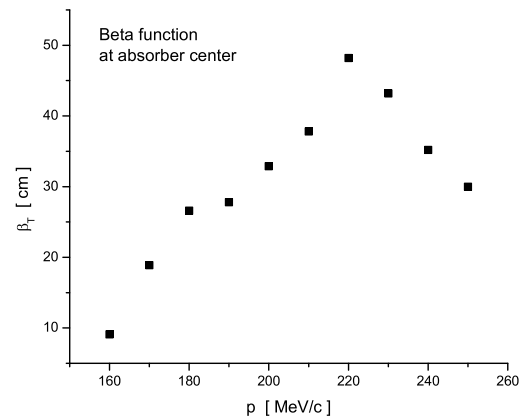


Figure 3: Magnetic field on axis for one cell. The upper panel is B_x ; the second one is B_y with average value of 0.125 T and the lower panel is B_s vs. distance.

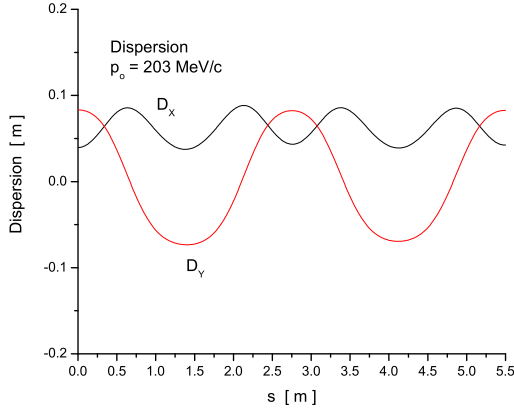


a)

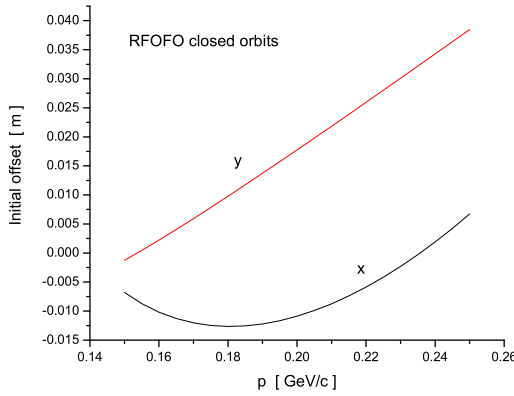


b)

Figure 4: a) Beta function vs. position in the cell; b) beta function as function of the muon momentum.



a)



b)

Figure 5: a) Dispersion vs. position in the cell; b) dispersion as function of the muon momentum.

tant field by summing the fields from a system of current sheets[6, 7]. The field of a solenoidal current sheet can be written analytically in terms of elliptic integrals. The resultant field components were shown to satisfy the 3D Maxwell equations to a high level of accuracy and agreed with independent calculations[8, 9]. The solenoidal field on-axis was approximately sinusoidal with a peak magnitude of 2.7 T. The solenoids were tipped to produce an average vertical dipole field of 0.125 T on-axis, as shown in Fig. 3. The circle containing the centers of the solenoids was displaced 10 cm outwards radially from the nominal beam axis in order to minimize the horizontal dipole field on the axis.

The rf cavities were modeled using cylindrical pillboxes running in the TM010 mode. The cavities are located in a dipole field in this design. Since we are accelerating muons, the cavities can be enclosed with metallic end windows in order to produce the maximum electric field on-axis for a given amount of rf power. The rf windows were stepped in thickness radially, in order to provide minimum thickness near the beam axis and still control the temperature increase due to rf heating.

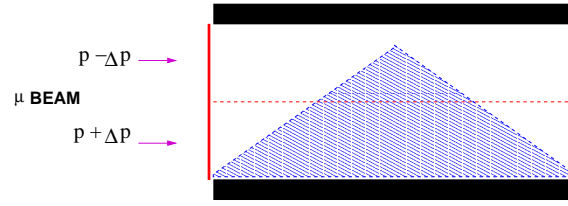


Figure 6: Wedge absorber used in the simulations.

The *wedge* absorbers are house-shaped, as shown in Fig. 6. The wedge only extends part way across the gap, such that a particle on the reference orbit always loses the same amount of energy crossing the wedge. The absorber windows were planar and located axially just in front of and behind the wedge itself. This is likely a worst case because the whole beam is forced to cross the window regardless of its transverse position. In reality the window shape will conform to the absorber and the effect on the beam of scattering in the window should be lessened.

We use a Gaussian input beam[8] in the simulations with a normalized transverse emittance of 12 mm and a normalized longitudinal emittance of 18.4 mm. The reference momentum is 203 MeV/c. This value was chosen to make the circulation time around the ring on a closed orbit equal to the 25th harmonic of 201.25 MHz. The initial beam has a correlation between the axial momentum and the transverse amplitude, to minimize the tendency for the particles in the bunch to spread out longitudinally in the solenoidal field. The initial *rms* bunch length is 8 cm, so this ring is not compatible with the bunch train assumed in Study-2. The use of compact cooling rings will likely also require the use of a preceding bunch compression ring.

The mean transverse position of the starting bunch was displaced by -10 mm in *x* and 18 mm in *y* to put the reference momentum particle on a closed orbit.

SIMULATION RESULTS

Merit Factors

Three merit factors have been widely used in the discussion of cooling ring performance. The quantity **M-factor**, defined by $M = \frac{\epsilon_6(\text{initial})}{\epsilon_6(\text{final})} \times \text{Transmission}$, explicitly combines the changes in 6D emittance and particle losses. This quantity is most useful for collider applications. Another figure of merit, which is local in character, is the **Q-factor** defined by $Q(s) = \frac{d\epsilon_6(s)/ds}{dN(s)/ds} \frac{N(s)}{\epsilon_6(s)}$; if $Q(s)$ is constant, then $\langle Q \rangle = \text{Ln}(\frac{\epsilon_6(s)}{\epsilon_6(0)}) / \text{Ln}(\frac{N(s)}{N(0)})$. This quantity essentially shows how efficiently the 6D emittance is reduced compared to particle losses. The third merit factor, and the one most directly useful for neutrino factories, is the muon density into a fixed accelerator acceptance volume. If N is the number of muons and V is a fixed acceptance volume in phase space, then we define the **D-factor** at any location s

along the ring to be $D(s) = \frac{N(s)/V(s)}{N(0)/V(0)}$.

Performance

We first consider the performance of an idealized ring, by which we mean a ring before the introduction of windows around the absorbers and rf cavities and before the introduction of empty cells for injection/extraction. Figure 7 shows the three emittances, transverse, longitudinal and 6D, merit factor M and transmission plotted on a logarithmic scale versus distance traveled. Table 2 summarizes the performance. The **M-factor** is 125, the **Q-factor** is 8.7 and the **D-factor** is 8.57.

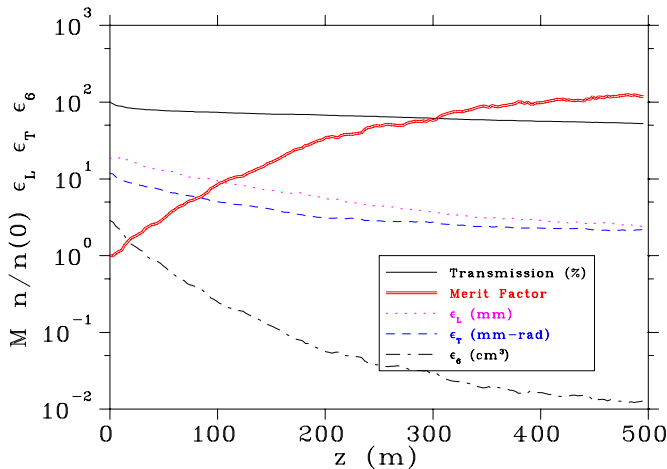


Figure 7: Performance of RFOFO Ring. Transmission, normalized transverse emittance, normalized longitudinal emittance, normalized 6-dimensional emittance, and the merit factor M, as a function of distance.

Table 2: RFOFO Ring Performance

	Before	After	ratio
ϵ_{\perp} (πmm^2)	11.87	2.14	5.5
ϵ_{\parallel} (πmm)	18.64	2.53	7.4
ϵ_6 ($\pi^3\text{cm}^3$)	2.86	0.012	238
N/N_0 , inc. decay	1	0.53	0.53
M-factor	1	125	125
D-factor	1	8.57	8.57

Initially, the ϵ_x emittance falls more rapidly than ϵ_y because it is the ϵ_y emittance that is exchanged with the longitudinal, but the Larmor rotations in the solenoidal field soon mix both emittances, bringing them to a common value.

After a distance of 400 m (≈ 12 turns), the 6D emittance has fallen by a factor of 238, with a transmission of 53% (66% without decay). The merit factor M is 125. The same factor for the Study-2 cooling lattice, also without windows, is 15.

We next show the idealized ring behavior in terms of the muon density. Figure 8 shows the total muon transmission together with the muon density into two fixed acceptance volumes. These volumes could correspond to the acceptance of a linear accelerator that follows the cooling ring at a neutrino factory.

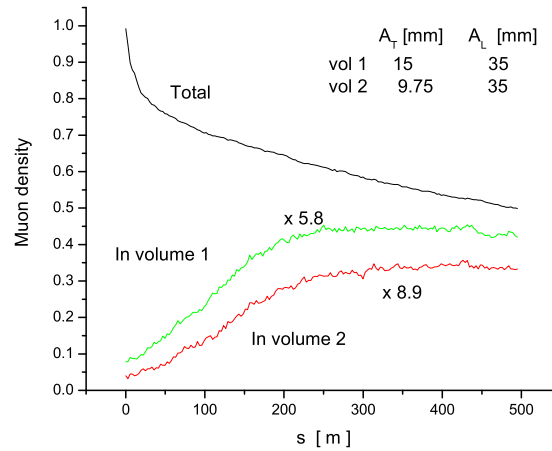


Figure 8: Performance of RFOFO Ring. Transmission and muon density into two fixed acceptance volumes. These results were obtained using a 100° wedge.

The idealized ring increases the muon density into the smaller acceptance volume by a factor of almost 9 in 250 m, which corresponds to about 8 turns. The density in the larger acceptance volume increases by about a factor of 6.

The introduction of windows around the absorbers or rf cavities introduces new sources of scattering and degrades the cooling performance. In addition a real ring needs space for injection/extraction. This is treated here by leaving the rf and absorbers out of two of the 12 lattice cells. The empty cells have the same pairs of solenoids however, so the magnetic field periodicity is preserved. Table 3 shows the result of a) adding absorber windows, b) adding rf cavity windows, and c) leaving empty cells in the lattice.

The absorber window used in Study-2 was $360 \mu\text{m}$ of aluminum. We see that windows of this thickness degrade the performance by about 30%. For safety reasons it may be necessary to use an additional window that increases the total amount of aluminum. On the other hand the use of other materials or optimized window shapes could reduce the amount of material. Another possibility would be to replace the liquid H_2 absorber with a solid material. LiH is one possible candidate, although Tb. 3 shows there is a 45% loss of performance with this option.

In Study-2 the Be end windows on the rf cavities were $200 \mu\text{m}$ thick from the axis out to a radius of 12 cm, then $400 \mu\text{m}$ thick out to 18 cm. The interior windows were $700 \mu\text{m}$ thick from the axis to a radius of 14 cm, then

Table 3: Perturbations on the idealized ring performance. FS2 stands for Study-2 used windows; FS2/20 stands for windows used in Study-2 with thicknesses reduced by a factor of 20.

absorber	abs win	rf win	empty cells	D
LH	none	none	0	8.93
LH	250 μm AL	none	0	7.50
LH	360 μm AL	none	0	6.60
LH	500 μm AL	none	0	6.08
LH	none	none	0	4.88
LH	none	FS2	0	5.88
LH	none	FS2/20	0	7.80
LH	none	none	2	6.73
LH	360 μm AL	FS2/20	2	4.25

1400 μm thick out to 21 cm. These windows degrade the performance by about 35%. One possibility to get around this problem is to operate the cavities at liquid nitrogen temperature. The lower operating temperature and the reduced rf gradient of 12 MV/m versus 16 MV/m in Study-2 allow the thickness of the windows to be decreased by a factor of 20 and the performance loss is only 13%. Alternatively, one could eliminate the rf cavity windows altogether and use an open cavity. This has the disadvantage that four times more power is required to produce the same E_z on axis.

Introducing empty cells for injection/extraction reduces the performance by 25%.

Finally, we consider an example that combines all of these effects. We choose liquid H_2 as the absorber with Study-2 like windows, assuming we can use this effective amount of aluminum because of improved alloys or window shape. We assume operation at liquid nitrogen temperature and use the thinner Be rf windows and leave empty cells in the lattice for injection/extraction. This realistic ring model still gives an impressive increase in the muon density of a factor of 4.25

REFERENCES

- [1] S. Ozaki, R. Palmer, M. Zisman, J. Gallardo, Editors, *Feasibility Study II of a Muon Based Neutrino Source*, BNL-52623, June, 2001.
- [2] The MC Collaboration, *Recent Progress in Neutrino Factory and Muon Collider Research within the Muon Collaboration*, to be published (<http://www.cap.bnl.gov/mumu/pubs/prstab-020814/prstab-rev1.pdf>)
- [3] R. Palmer, Ring coolers, in Proc. NuFact02 Workshop, London, July 2002.
- [4] J.S. Berg, R.C. Fernow, R.B. Palmer, *An Alternating Solenoid Focused Ionization Cooling Ring*, MUC-NOTE-COOL-THEORY-239, Mar. 2002. This series of technical notes can be found at (<http://www-mucool.fnal.gov/mcnotes/>)

- [5] R. Fernow, *ICOOL: a simulation code for ionization cooling of muon beams*, Proc. 1999 Particle Accelerator Conference, p. 3020-3022.
- [6] R. Fernow, J. Gallardo, *Realistic on-axis fields for the RFOFO cooling ring*, MUC-NOTE-COOL-THEORY-265, Nov. 2002.
- [7] R. Fernow, J. Gallardo, *Calculation of RFOFO fields using the off-axis expansion in ICOOL*, MUC-NOTE-COOL-THEORY-268, Jan. 2003.
- [8] V. Balbekov, *Simulation of RFOFO ring cooler with tilted solenoids*, MUC-NOTE-COOL-THEORY-264, Nov. 2002.
- [9] S. Bracker, *Magnetic field maps for the RFOFO muon cooling ring*, MUC-NOTE-COOL-THEORY-271, Mar. 2003.